International Journal of Geosciences, 2013, 4, 1200-1214
http://dx.doi.org/10.4236/ijg.2013.48114 Published Online October 2013 (http://www.scirp.org/journal/ijg)

Some Notes on the Lugiin Gol, Mushgai Khudag and Bayan Khoshuu Alkaline Complexes, Southern Mongolia

Munkhtsengel Baatar[1*], Gerel Ochir[1], Jindrich Kynicky[2], Shigeru Iizumi[3], Piero Comin-Chiaramonti[4]
[1]Department of Geology, Mongolian University of Science & Technology, Ulaanbaatar, Mongolia
[2]Department of Geology and Pedology, Mendel University, Brno, Czech Republic
[3]Department of Geosciences, Shimane University, Matsue, Japan
[4]Department of Mathematics and Geosciences, Trieste University, Trieste, Italy
Email: *munkhtsengel@yahoo.com

Received July 16, 2013; revised August 19, 2013; accepted September 22, 2013

ABSTRACT

Volcanic-plutonic alkaline complexes from Lugiin Gol, Mushgai Khudag and Bayan Khoshuu, southern Mongolia (244, 139 and 131 Ma, respectively) occur within grabens in E-W lineaments. They are represented by syenitic rock-types (silica undersaturated to slightly silica oversaturated) potassic rocks and are associated to stockworks of carbonatitic veins, dykes and so on. Geochemical characteristics and isotope systematics point to a veined mantle source particularly enriched in LILE and LREE. The carbonatitic veins show high contents of Ba, Sr, Th and REE and are suitable as potential ore deposits.

Keywords: Mongolia; Alkaline Complexes; Carbonatites; REE Deposits

1. Introduction

Alkaline province in Southern Mongolia is well known for associated alkaline-carbonatite complexes (e.g. Lugiin Gol, Mushgai Khudag and Bayan Khoshuu) (**Figure 1**). These complexes and a number of smaller plutons with carbonatite dykes and veins are controlled by E-W faults and formed in continental rift environment. Alkaline and carbonatitic rocks [1-7] outcrop along the northern and south Gobi rift zones (Late Paleozoic to Early-Late Mesozoic aged) and consist mainly of volcanic-plutonic complexes.

We present here a review of the petrological and geochemical features of these alkaline-carbonatite complexes.

2. Geological Background

The alkaline complexes in South Mongolia are controlled by large extensional structures (**Figure 1**) and are related to occurrences of Late Paleozoic-Early Mesozoic (Lugiin Gol) and Late Mesozoic (Mushgai Khudag and Bayan Khoshuu) ages, respectively ([8], and therein references).

2.1. Lugiin Gol Complex (LGC)

LGC outcrops at the Southeastern side of the Gobi-Tien Shan fold belt, near the boundary with the Sulinkheer suture zone (**Figure 1**). Gobi-Tien Shan belt is composed mainly of Late Pre-Cambrian limestones, amphibolites and gneisses with Late Paleozoic granitoids and intermediate volcanics. The Sulinkheer zone is characterized by a Paleozoic ophiolitic complex and by Late Paleozoic sediments, in the southern and in the northern areas, respectively. The eastern Lugiin Gol district (108˚20'E) represents a magmatic arc, indicating that remnant oceanic basin (Sulinkheer Sea) existed between North China and a South Gobi microcontinent until Late Permian [9,10].

Notably, the northern area is mainly underlain by black shales, siltstones and sandstones (*i.e.* Lugiin Gol Formation), intruded by the LGC complex. A silica undersaturated syenitic stock outcrops in an area of about 12 sq.km, showing subcircular outlines with a diameter of 3.5 km. The stock is composed of nepheline-bearing syenite, nepheline syenite and ijolites (**Figure 2**), surrounded by hornfels [4,11], fenites and skarns. An alkali-granite dyke, 20 m thick, crosscuts the Lugiin Gol complex. Moreover, a stockwork with two main types of dykes and veins, *i.e.* carbonatites and phonolites (and phonolites with tinguaitic texture) intrude the complex (cf. **Figure 2**).

*Corresponding author.

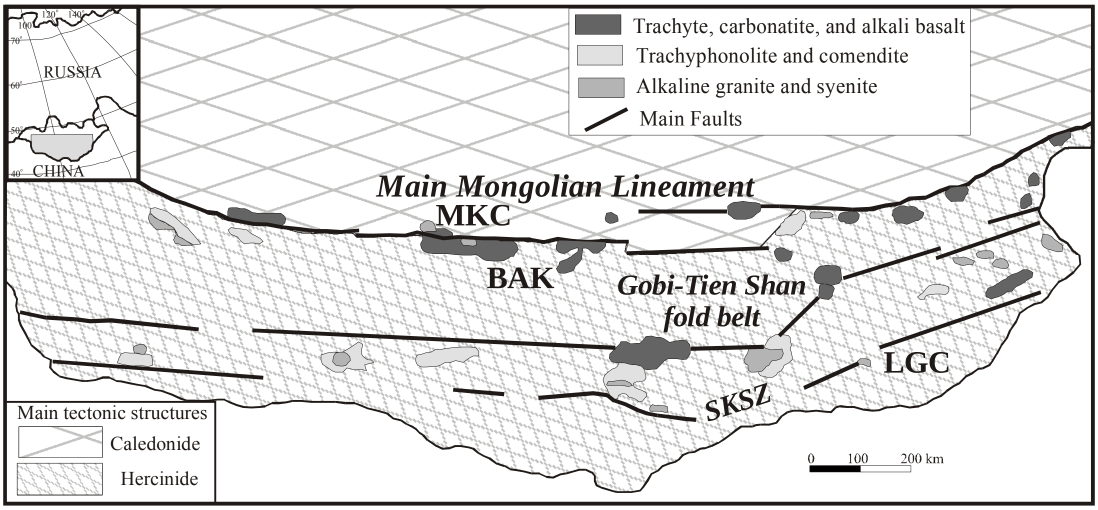

Figure 1. Distribution of alkaline complexes in South Mongolia [3]: MKC, Mushgai Khudag; BAK, Bayan Khoshuu; LGC, Lugiin Gol; SKSZ, Sulinkheer suture zone. Grey field in the inset represents the studied area.

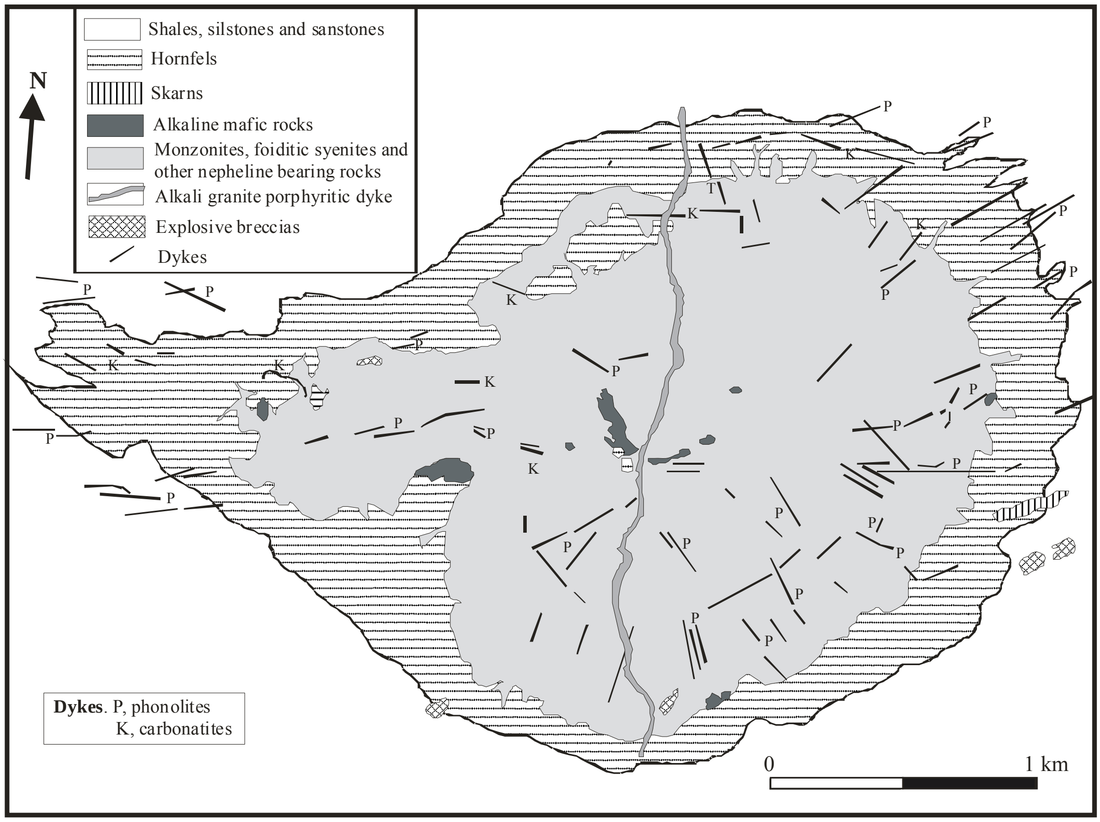

Figure 2. Lithological map of the Lugiin Gol complex [4,12]. Only significant occurrences of carbonatitic dykes and veins are shown.

2.2. Mushgai Khudag Complex (MKC)

MKC, along the main Mongolian lineament (**Figure 1**) consists mainly of stocks and necks of trachytic and syenitic varieties (**Figure 3**; [13] cut by carbonatitic veins and plugs (F-S-Sr-Ba-REE rich: s. later). Host rocks are represented by Paleozoic sedimentary-volcanic sequences and by Carboniferous granitoids [3]. The K-Ar ages for MKC are between Early Cretaceous (Valanginian) and Late Cretaceous (Cenomanian) times [5].

Genesis of these rocks was interpreted as a result of a mantle plume activity during subduction (Enkhtuvshin, 1995), or, more probably, as rifting related [3].

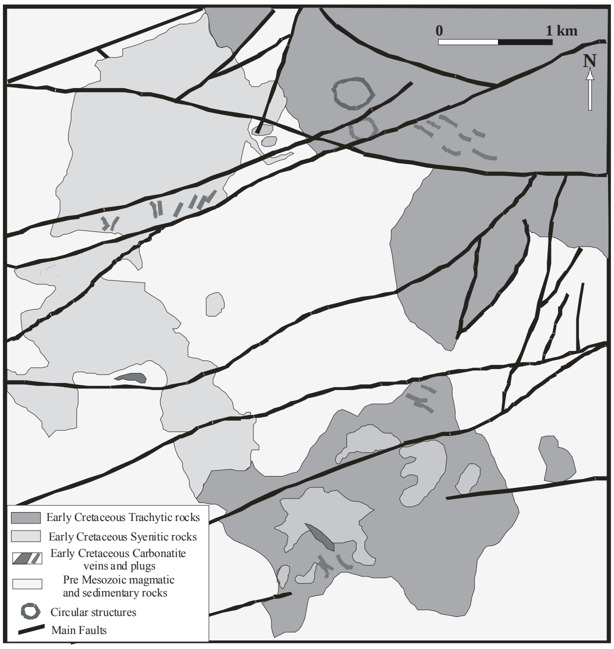

Figure 3. Simplified geological map of the Mushgai Khudag Complex (Latitude: 44˚24'3"N, Longitude: 104˚3'5"E) after [3].

2.3. Bayan Khoshuu Complex (BAKC)

BAKC consists of Late Jurassic to Early Cretaceous trachytes, syenites and monzonites. Late Paleozoic syenites, granites and Silurian volcanic-terrigenous rocks represent host rocks. Syenites and monzonites occur at the core of the complex. Carbonatitic stockworks are noticeable (**Figure 4**).

Several primary and hydrothermal mineralizations (F-S-Sr-Ba-REE rich; cf. [14]) are present mainly as veins intruding the rocks.

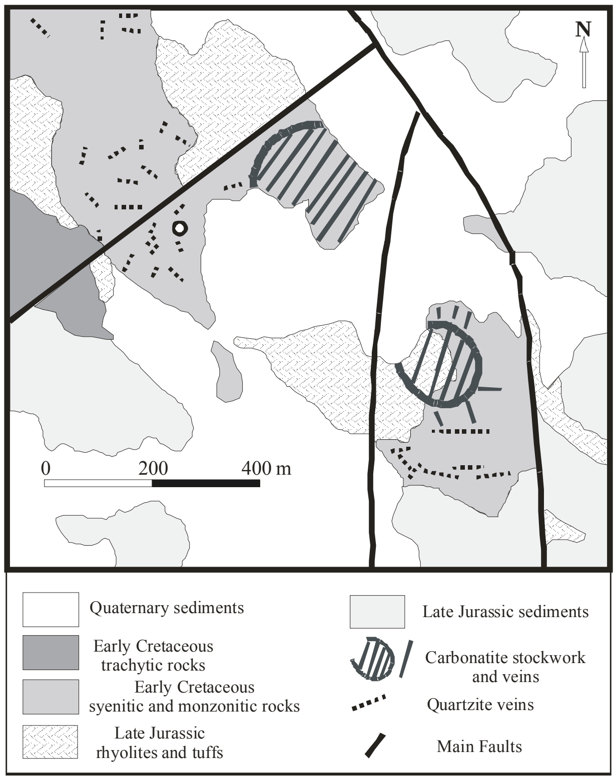

Figure 4. Geological map of the bayan khoshuu complex (modified, after [15]).

3. Petrographical Outlines

3.1. Silicate Rocks

The petrography is based here above all on the [16] and [17] classifications.

The *foid* (*nepheline*) *syenites* are medium to coarse grained, equigranular to subporphyritic. Major minerals are orthoclase (or ≥80 mole%), nepheline, clinopyroxene (usually with augitic-diopsidic core and aegirine-rich rims). Minor minerals are amphibole (arfvedsonite with Mg# ~0.65), biotite, titanite, fluorite, sodalite, calcite, magnetite and apatite. As typical accessory minerals occur zircon, baddeleyite, elpidite, pyrochlore, burbankite, cancrinite and synchysite.

Foid bearing monzonites (*syenites*) are porphyritic with euhedral phenocrysts of alkali feldspar and plagioclase set in a matrix of clinopyroxene, amphibole, biotite and nepheline: accessory minerals are magnetite, titanite, apatite and zircon.

Porphyritic fine- to medium-grained K-feldspar *monzonites and syenites* are composed of K-feldspar, plagioclase, clinopyroxene (augite to diopside $Wo_{48-37}En_{40-20}Fs_{13-21}$), alkaline amphibole (Mg arfvedsonite with Mg # = 60 - 70), biotite ($Ann_{0.6-0.76}$), magnetite, quartz, plagioclase and accessory apatite, titanite and fluorite.

Phonolites with tinguaitic texture (*Tinguaites*, *i.e.* "intrusive phonolites") are usually porphyritic, with phenocrystals of alkali feldspar, nepheline, biotite and aegirine-augite ± sodic amphibole, being titanite and aegirine the most common inclusions. The groundmass is a fine aggregate of nepheline, alkali feldspar, biotite, aegirine, titanite, apatite, magnetite and zircon. Notably, needles of aegirine occur interstitially in a mosaic of alkali feldspar and foids ("tinguaitic texture"; cf. [17]. The associated *phonolites* are very fine grained, sometimes porphyritic, with the same mineralogical association of the coexisting tinguaites.

The *granitic dyke* of the Lugiin Gol complex is mainly course, but locally also very coarse, with large phenocrysts of microcline, oligoclase, biotite and quartz set in a groundmass made of the same phases. Accessory minerals are mainly amphibole, titanite, apatite, magnetite and ilmenite.

3.2. Carbonatites

According to Kynicky and Samec [11] and Kynicky *et al*.

[18,19], the carbonatites are mainly sővite and alvikite, consisting essentially of calcite, minor to accessory apatite and fluorite, fluorcarbonates, strontianite, barite, celestine and quartz. The textures of examined carbonatites usually show a recrystallization of magmatic calcite, alteration of apatite, and crystallization of minerals controlled by the intensity of hydrothermal-metasomatic alteration [14,20,21]. It is suggested that there are two types of alteration in the carbonatites: 1) high temperature (above 250˚C, max 400˚C) fluoritization with crystallization of fluorocarbonates (e.g. bastnaesite-(Ce), synchysite-(Ce), Ce- and Nd-parisite); 2) low temperature (bellow 150˚C) with crystallization of barite, celestine and quartz (up to the stage IV of [22]).

Notably, carbonatites usually form veins within magmatic rocks, or they are mainly located in brecciated rocks and eruptive breccias. There are rare crater facies at the contact of syenite plutons [3]. On the whole the carbonatitic rocks from the three complexes are similar, but Mushgai Khudag complex shows relatively high concentrations of apatite, and barite-celestine as well fluorocarbonates may be important in the veins from Bayan Khoshuu complex.

4. Petrochemistry

4.1. Classification and Nomenclature

The classification and nomenclature is after the TAS [17,23,24] cf. **Figure 5(a)**), and on the basis of QAPF diagram [16]. The silicate rocks of the analyzed complexes are rich in alkalis, with total alkali content (Na_2O + K_2O) ranging from 10.1 to 16.7 wt% (cf. **Tables 1** and **2**): on the basis of the Na_2O/K_2O ratio they are "potassic"; only one phonolitic (tinguaitic) dyke from Lugiin Gol complex plots inside the "highly potassic" field (**Figure 5(b)**). Agpaitic index ranges from 0.76 to 1.18 pointing to a tendency towards peralkaline rock-types. Silica and MgO contents range from 52.0 to 58.7 and from 3.48 to 0.11 wt%, respectively, indicating that the rocks are evolved (from intermediate to acid, following) [23]. Analogously to similar occurrences, the rocks may derive, via fractional crystallization, by original basanitic magmas [22,25,26].

The analyzed samples (**Tables 1** and **2**), plotted in the TAS (**Figure 5(a)**), are: 9 foid syenites, 5 foid bearing monzonites, 1 monzonites, 2 phonolites, 6 phonolites with tinguaitic texture, 7 monzonites and 2 syenites, other than the alkali granite dyke (4 samples) of the Lugiin Gol complex.

Following the Q-A-P-F classification, where the distribution of the Ab molecule between alkali feldspar and plagioclase was obtained according to Le Maitre (1976) on the CIPW norms (**Figure 5(c)**), the samples are foid-syenites/phonolites and foid bearing syenites/trachytes (Lugiin Gol) and syenites/trachytes (Mushgai Khudag and Bayan Khoshuu).

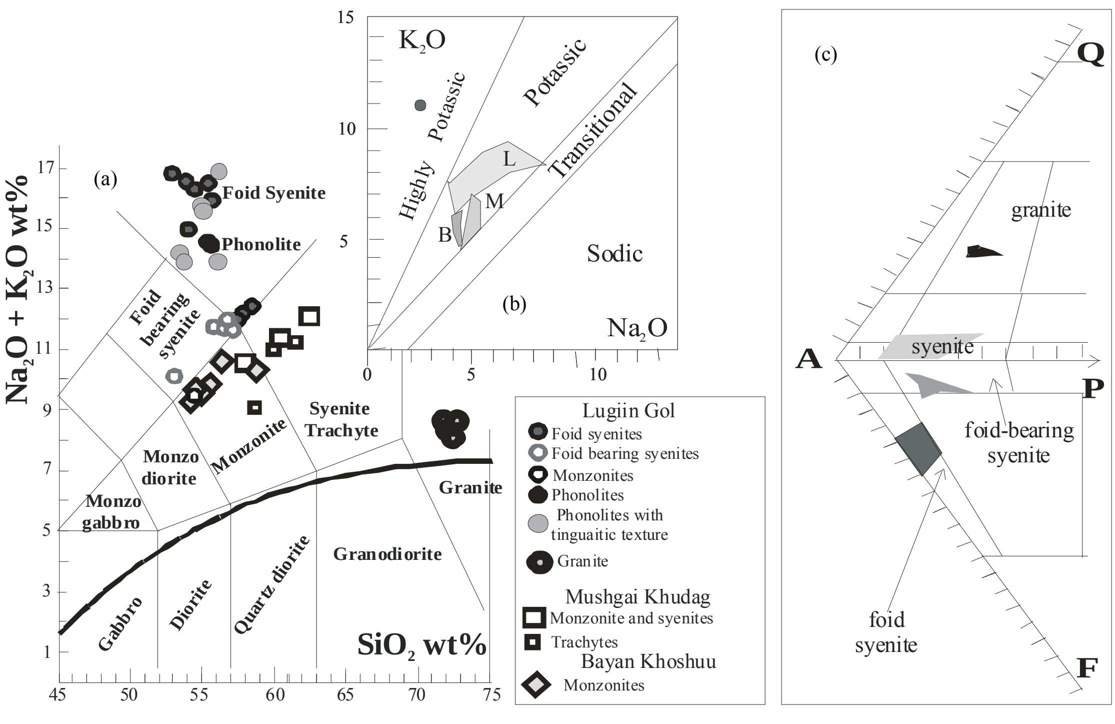

Figure 5. (a) Total alkali-silica diagram, TAS, modified after Middlemost, 1994. Heavy line separates alkaline and subalkaline fields [27]; (b) Na_2O vs K_2O diagram; L, Lugiin Gol, M, Mushgai Khudag, B, Bayan Khoshuu; (c) In the Q-A-P-F diagram [16] the normative values were plotted after the sharing out Ab between alkali feldspar and plagioclase [28].

Table 1. Major element concentrations (wt%) for the Lugiin Gol selected samples and relative CIPW norms. APF calculated following [28]. Major elements were analyzed by XRF fluorescence techniques at the Shimane University, Japan (Department of Geosciences, Lagoon Research Center); FeO contents were determined by the $KMnO_4$ solution titration method. Nomenclature according to QAPF of [16,29]. A.I.: agpaitic index, molecular ratio of ($Na_2O + K_2O$)/Al_2O_3.

Foid syenite (Foids = 34.5% - 22.5%) and foid-bearing syenite to foid monzosyenite (Foids = 10.6% to 3.3%)															
Sample	82311	82307	82314	82315	82302	82303	70512	82306	70507	82301	82312	82313	82308	82304	82316
SiO_2	55.27	54.65	53.60	52.98	55.66	54.10	54.31	57.21	53.13	56.90	56.03	57.84	58.67	56.49	57.23
TiO_2	0.23	0.21	0.36	0.39	0.16	0.43	0.48	0.48	0.94	0.45	0.41	0.49	0.45	0.51	0.52
Al_2O_3	21.43	20.90	20.18	19.90	21.45	21.24	20.11	18.33	17.46	17.75	18.60	18.19	18.49	17.86	17.45
Fe_2O_3	1.10	1.29	1.80	2.06	1.20	2.33	1.66	2.17	1.64	1.85	1.77	1.47	2.24	2.49	1.99
FeO	0.74	1.34	0.85	0.96	0.53	1.76	2.39	3.02	5.39	3.93	3.55	3.49	1.72	2.92	3.87
MnO	0.07	0.14	0.14	0.16	0.08	0.16	0.15	0.16	0.22	0.22	0.19	0.13	0.12	0.18	0.18
MgO	0.12	0.17	0.16	0.21	0.16	0.29	0.70	0.82	2.48	0.88	0.74	0.83	0.74	0.95	1.34
CaO	1.39	1.82	2.08	2.34	1.92	2.11	3.06	2.90	5.69	3.70	3.12	2.94	2.67	3.33	3.70
Na_2O	7.32	6.88	8.37	8.28	6.72	6.66	6.40	4.86	4.00	4.68	4.40	4.60	4.55	4.89	3.78
K_2O	9.16	9.31	8.35	8.42	9.08	8.26	7.89	7.05	6.11	7.21	7.43	7.43	7.83	6.76	7.60
P_2O_5	0.03	0.04	0.03	0.15	0.05	0.03	0.20	0.20	0.53	0.18	0.18	0.20	0.18	0.22	0.26
LOI	2.51	2.46	3.57	3.38	2.25	1.84	1.76	1.97	1.51	1.97	3.09	1.66	1.70	2.99	1.30
Total	99.37	99.21	99.49	99.23	99.26	99.21	99.11	99.17	99.10	99.72	99.51	99.27	99.36	99.59	99.22
A.I.	1.02	1.02	1.13	1.14	0.97	0.94	0.95	0.85	0.76	0.87	0.82	0.86	0.86	0.86	0.83
or	54.13	55.02	49.35	49.76	53.66	48.82	43.67	41.66	36.11	42.61	43.91	43.91	46.81	40.44	44.91
ab	6.29	4.50	9.09	7.49	11.60	12.60	16.50	21.30	20.02	26.46	25.79	29.44	30.93	33.19	27.07
an	-	-	-	-	-	3.67	4.32	-	11.64	6.13	9.06	7.96	6.64	6.90	8.20
ne	28.68	27.72	26.13	26.00	24.52	23.70	20.40	18.28	7.49	7.12	6.20	5.14	4.10	2.66	2.66
ac	2.38	2.24	0.91	0.91	-	-	-	4.07	-	-	-	-	-	-	-
ns	-	-	2.90	3.13	-	-	-	-	-	-	-	-	-	-	-
di	2.30	4.58	0.91	1.13	-	3.24	8.06	11.06	10.93	9.42	4.48	4.52	4.38	6.96	7.09
wo	1.99	1.46	3.74	3.72	2.73	1.13	-	-	-	-	-	-	-	-	-
ol	-	-	-	-	-	-	0.17	0.25	6.14	2.06	3.23	3.66	0.37	1.28	3.48
mt	0.40	0.75	2.15	2.49	1.50	3.38	2.41	1.11	2.38	2.68	2.57	2.13	3.25	3.61	2.89
il	0.43	0.40	0.68	0.74	0.30	0.82	0.91	0.91	1.78	0.85	0.78	0.93	9.83	0.97	0.99
hm	-	-	-	-	0.16	-	-	-	-	-	-	-	-	-	-
ap	0.07	0.09	0.07	0.35	0.12	0.07	0.46	0.46	1.23	0.42	0.42	0.46	0.42	0.51	0.60
A	67.8	68.2	66.8	65.5	72.6	72.1	65.5	77.5	68.1	78.2	76.9	79.6	83.6	80.9	81.8
P	0..0	0.0	0	0.0	0.0	4.5	6.7	0.0	22	11.2	15.8	14.4	11.8	13.8	14.9
F	32.2	31.8	33.2	34.5	27.4	23.4	27.8	22.5	9.9	10.6	7.3	6.0	4.6	5.3	3.3

	Phonolite dykes with tinguaitic texture					Phonolite dykes			Alkali granite porphyry dyke				Carbonatite dykes			
Sample	82317	70508	70510	70504	70509	70506	70516	70517	70514	82305	82309	70515	70503	71504	LG-07	LG-11
SiO_2	53.80	53.59	56.12	54.86	54.90	55.82	55.68	55.22	72.38	72.15	72.22	72.35	4.85	6.74	10.92	3.23
TiO_2	0.82	0.81	0.46	0.29	0.33	0.18	0.45	0.46	0.23	0.23	0.23	0.23	0.01	0.32	0.65	0.04
Al_2O_3	19.31	19.34	20.89	19.91	20.62	19.71	21.03	20.55	14.00	13.89	13.98	13.95	1.30	0.82	0.38	0.25
Fe_2O_3	2.57	2.00	1.34	1.91	0.96	2.64	1.91	1.96	1.29	1.23	0.66	0.72	1.42	1.89	2.30	1.70
FeO	2.03	2.44	2.27	1.36	1.68	0.42	1.12	1.56	0.49	0.56	1.00	0.98	0.06	n.d.	n.d.	n.d.
MnO	0.16	0.16	0.15	0.16	0.12	0.17	0.14	0.15	0.06	0.04	0.06	0.05	1.64	1.60	1.49	0.65
MgO	0.97	0.94	0.69	0.22	0.16	0.11	0.42	0.46	0.67	0.61	0.48	0.48	3.95	1.64	0.83	0.43
CaO	3.78	3.77	3.10	2.21	1.97	1.41	2.17	2.42	1.36	1.36	1.69	0.96	47.44	45.55	45.97	50.93
Na_2O	6.39	6.27	2.35	7.76	7.58	8.61	5.52	5.93	3.03	3.28	3.21	3.41	n.d.	0.01	0.02	0.20
K_2O	7.39	7.65	10.91	8.00	8.00	8.38	8.88	8.64	5.00	4.95	4.92	4.88	0.28	0.49	0.15	0.16
P_2O_5	0.29	0.28	0.18	0.03	0.04	0.01	0.12	0.13	0.06	0.06	0.06	0.06	0.11	0.19	0.18	0.03
LOI	2.02	1.83	0.98	2.84	2.46	1.98	1.93	1.97	2.27	1.98	2.04	2.49	38.40	37.53	30.87	33.79

Continued

Total	99.53	99.08	99.45	99.55	98.82	99.44	99.37	99.45		100.84	100.34	100.55	100.56	99.46	96.78	93.8	91.4
A.I.	0.96	0.96	0.75	1.08	1.03	1.18	0.89	0.93		0.74	0.77	0.76	0.78				
Q	-	-	-	-	-	-	-	-		31.79	30.42	29.92	30.65				
C	-	-	-	-	-	-	-	-		1.20	0.77	0.30	1.31				
or	43.67	45.21	64.48	47.28	47.28	49.52	52.48	51,17		29.55	29.25	29.08	28.84				
ab	15.97	14.19	5.60	8.83	11.86	9.00	14.90	13.94		25.64	27.76	27.16	28.86				
an	2.18	2.03	14.21	-	-	-	6.38	3.94		6.55	6.47	8.39	4.76				
ne	6.24	21.06	7.74	27.39	26.91	24.77	17.23	19.63		-	-	-	-				
ac	-	-	-	5.53	2.31	7.64	-	-		-	-	-	-				
ns	-	-	-	-	-	2.20	-	-		-	-	-	-				
di	6.24	6.39	-	5.48	5.80	2.08	2.26	3.91		-	-	-	-				
wo	2.85	3.24	-	1.82	1.31	1.88	0.29	1.01			-	-	-				
hy	-	-	-	-	-	-	-	-		1.93	1.52	2.22	2.11				
ol	-	-	3.20	-	-	-	-	-		-	-	-	-				
mt	3.73	2.90	1.94	-	0.24	-	2.76	2.84		1.11	1.29	0.96	1.04				
il	1.56	1.54	0.87	0.55	0.63	0.34	0.85	1.15		0.43	0.43	0.43	0.43				
hm	-	-	-	-	-	-	0.03	-		0.53	0.35	-	-				
ap	0.67	0.65	0.42	0.07	0.09	0.02	0.28	0.30		0.10	0.10	0.10	0.10				
A	71.4	71.3	75.1	67.2	68.7	68.5	72.3	72.3	Q	34.0	32.4	31.6	32.9				
P	3.6	3.2	16.5	0.0	0.0	0.0	8.8	5.6	A	54.0	55.4	51.31	57.6				
F	25.0	25.5	8.4	32.8	31.3	31.5	18.9	22.1	P	12.0	12.2	15.3	9.5				

Representative analyses of Ca-carbonatites are reported in the **Tables 1** and **2**, along the analyses of F-REE rich variants from the Bayan Khoshuu complex.

4.2. Geochemistry

Notably, all the Lugiin Gol samples, granitic dyke excepted, are Ne normative (Ne 2.66 to 28.68 wt%; cf. **Table 1**), whereas the alkaline rocks from the Mushgai Khudag and Bayan Khoshuu are oversaturated or saturated in silica (Q = 0.0 to 7.6 wt%; cf. **Table 2**). All the samples display a variable Al_2O_3 content (14.74 - 17.96 wt%). On the whole, the rocks appear enriched in LILE and depleted in HFS elements such as Nb, Ta, P and Ti. They show a strongly enriched pattern in Pb (**Tables 3**, **4** and **Figure 6**). On the other hand, the rocks are enriched in LREE and depleted in HREE (showing flat patterns), with a weak negative Eu anomaly (**Tables 3**, **4** and **Figure 7**).

In particular, the carbonatite dykes and veins from the complexes (**Figure 7** and **Tables 3**, **4**) show a very high concentration of U, Th, (up to 3843 and 114, ppm, respectively) and REE (REE = 0.6 - 3.3, up to 23.5 wt%; LREE = 6928 up to 224,291 ppm) and a very strong fractionation LREE/HREE (Nd/Lu = 854 - 24,100). It can be stressed that the highest values are typical of the later veins from Bayan Khoshuu complex and "high grade" carbonatites from Lugiin Gol complex, linked to the presence of fluorocarbonate minerals as bastnaesite, synchysite and parisite: this suggests an economic importance for these occurrences, almost for LREE (cf. also [30] and therein references). As matter of fact, from mass balance (**Tables 2** and **4**) the MK vein contains approximately barite 13 wt%, celestine + strontianite 17 wt% and bastnaesite + synchysite+ parisite (up to 28 wt%). Moreover, an exceptional content of apatite is present in the MK-01 carbonatite (about 13.5 wt%). Considering major and trace elements, REE contents of intrusive rocks from the Mushgai Khudag and Bayan Khoshuu complexes (shown in **Tables 2** and **4**), it is apparent that these rocks are strongly enriched in Sr, Pb and LILE and depleted in HFSE (Ta, Nb, Hf, Ti, and Y) (**Figure 6**). They show enriched LREE pattern (**Figure 7**). Geochemically these rocks are characterized by relatively low HFSE with enrichment in LILE and LREE, depletion in Ta, Nb, Ti and Zr with HFSE troughs on the primordial mantle normalized spiderdiagrams [31], which are commonly observed in island arc basalts and in the Paraná volcanic, the latter linked to extensional (rifting) processes [32]. It suggests that the original (basanitic?) magmas were derived from continental lithospheric, mantle, metasomatized by fluids, variably enriched in CO_2 and H_2O (and F, LILE and so on: cf. veined mantle of [33,34]. On the whole, all the data, suggest that the Mongolian alkaline complexes from southern Mongolia are related to the lithospheric mantle, where the contribution of asthenospheric components are not appreciable in terms of geochemical signatures (cf. [32], and therein

Table 2. Major element compositions (wt%) for selected intrusive samples from Mushgai Khudag and Bayan Khoshuu complexes. Effusive selected samples are from [5]; Fe_2O_3-FeO partitioning determined by Ox of [28]. Carbonatite dyke and F-carbonate veins are from[19] (unpublished data).

	Mushgai Khudag								Bayan Khoshuu							
	Intrusive			Effusive			Carbonatite dykes		Intrusive						F-Carbonate veins	
Sample	80801	90601	90703	80410	80408	80307-3	3/MK	MK-01	90706	90707	90704	90708	90709	90710	BK	BK-02
SiO_2	62.50	60.65	57.73	61.40	59.83	58.64	1.07	7.92	55.77	54.82	58.90	54.17	56.24	56.38	1.29	2.09
TiO_2	0.70	0.94	0.78	0.79	0.76	1.25	0.01	0.11	1.21	0.91	0.78	1.10	0.94	0.87	0.01	<0.01
Al_2O_3	15.72	15.99	16.10	17.96	17.34	15.29	0.10	1.23	14.31	14.38	14.76	14.38	14.40	14.91	0.25	0.49
Fe_2O_3	2.95	3.33	4.18	2.07	2.53	2.95	0.77	0.66	3.58	3.62	2.60	3.68	3.19	3.71	1.31	1.41
FeO	0.80	1.05	1.47	1.65	1.99	2.34	n.d.	n.d.	2.21	2.04	1.46	1.79	1.96	1.31	n.d.	n.d.
MnO	0.07	0.08	0.12	0.04	0.09	0.07	0.24	0.55	0.11	0.10	0.09	0.11	0.10	0.14	0.18	0.21
MgO	1.08	1.08	1.37	0.64	1.14	2.43	2.51	3.89	3.06	3.48	2.39	2.99	2.79	2.16	0.42	0.46
CaO	1.82	2.61	3.48	1.93	2.52	4.88	51.81	48.88	5.84	5.52	4.85	6.10	5.90	4.25	8.45	9.32
Na_2O	4.87	5.59	5.10	5.31	5.30	4.48	0.05	0.18	4.33	4.32	4.21	4.10	4.25	4.49	0.23	0.47
K_2O	7.13	5.72	5.60	6.03	5.75	4.51	0.07	0.40	4.85	5.23	6.10	5.42	5.66	6.25	0.16	0.22
P_2O_5	0.36	0.33	0.58	0.34	0.40	0.91	2.74	5.80	1.06	0.99	0.94	1.05	1.51	0.82	0.20	0.34
LOI	0.45	1.49	2.19	n.d.	n.d.	n.d.	39.00	25.03	2.23	3.08	1.50	3.44	1.90	3.60	16.28	20.69
Total	98.45	98.86	98.70	98.16	97.65	97.75	98.40	94.7	98.56	98.49	98.58	98.33	98.84	98.89	28.78	35.7
A.I.	1.00	0.96	0.90	0.85	0.86	0.80			0.86	0.89	0.84	0.88	0.91	0.95		
Q	4.73	2.94	1.54	3.26	1.51	5.97			0.29	0.00	3.17	0.00	0.93	0.11		
or	42.14	33.80	33.10	35.63	33.98	26.65			28.66	30.91	36.05	32.03	33.45	36.94		
ab	33.17	38.45	35.91	44.93	44.85	37.66			36.64	34.22	33.29	29.27	34.37	30.68		
an	4.24	6.34	8.34	7.36	6.54	8.43			5.28	5.59	4.60	7.71	4.35	5.94		
ac	7.08	7.80	6.37	-	-	0.26			2.43	1.97	2.06	4.78	1.41	6.43		
di	1.90	3.47	4.00	-	2.65	7.66			13.05	11.94	10.37	12.22	11.73	7.62		
hy	1.81	1.08	1.56	1.68	2.14	2.50			1.57	0.70	1.26	0.59	1.51	1.85		
mt	0.73	0.92	2.87	3.00	3.52	4,15			3.98	4.26	2.74	2.94	3.92	2.16		
il	1.33	1.78	1.48	1.50	1.44	2.37			2.30	1.73	1.48	2.09	1.78	1.65		
ap	0.83	0.76	1.34	0.79	0.93	2.11			2.46	2.29	2.18	2.43	3.50	1.90		
Q	5.6	3.6	2.0	3.6	1.7	7.6			0.4	0.0	4.1	0.0	1.3	0.2		
A	85.8	81.2	78.3	79.9	82.4	55.26			84.1	84.7	85.0	80.6	87.3	86.0		
P	8.6	15.2	19.7	16.5	15.9	22.2			15.5	15.3	10.9	19.4	11.4	13.8		

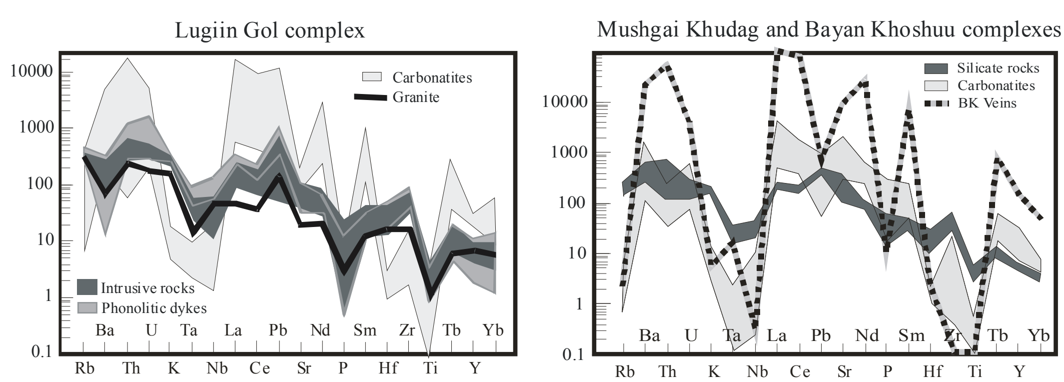

Figure 6. Primitive mantle normalized [31] spidergram for the Lugiin Gol, Mushgai Khudag and Bayan Khoshuu complexes.

Table 3. Trace element concentrations (ppm) for the Lugiin Gol selected samples; trace elements were determined by ICP-Mass Spectrometer (Shimane University) by alkali fusion and acid digestion methods; n.d., not determined. Nomenclature according to the TAS.

	Foid									Foid bearing			Monzonite	
Sample	82308	82313	82306	82302	82303	82315	82311	82307	82314	82301	82312	70507	82304	82316	70512
Cr	6	9	18	n.d.	n.d.	n.d.	n.d.	n.d.	n.d.	11	n.d.	53	13	21	1
Ni	8	8	11	n.d.	5	5	n.d.	4	4	12	9	15	10	9	7
Rb	226	204	247	174	165	200	177	220	160	247	241	174	223	214	237
Ba	876	992	674	938	533	781	624	504	514	490	684	2099	723	1224	2050
Th	23	20	28	15	33	34	8	51	55	45	51	21	27	40	40
U	8.4	6.3	6.8	5.1	5.9	13.9	n.d.	11	10.4	10.6	14.1	6.1	7.9	6.3	n.d.
Nb	27	27	28.8	8	19.3	41.9	n.d.	23.3	38.9	32.5	35.8	48.8	26.6	26.4	27
Ta	1.8	2.3	1.8	1.0	1.3	1.9	n.d.	1.2	2.2	2.0	2.3	2.4	1.6	1.6	n.d.
Sr	1212	1026	796	2182	1792	1955	1686	1211	1918	1119	791	2037	1218	1394	2440
Pb	99	70	81	49	76	131	58	79	93	99	83	80	83	58	55
Zr	99	70	81	49	76	131	58	79	93	99	83	80	83	58	55
Hf	8.1	10	7.7	4	5.1	4.7	n.d.	7	7.8	10.5	11.2	12.5	7.9	12.6	n.d.
Y	28	33	34	18	20	28	12	23	34	45	41	39	36	37	32
La	81	98	114	61	70	100	n.d.	119	103	164	140	131	138	149	n.d.
Ce	156	207	218	112.4	144	187	n.d.	215	201	334	276	263	269	310	n.d.
Pr	17	22.4	22.6	11.4	15	20	n.d.	20	21.4	33	29	29	26.5	31.1	n.d.
Nd	37.6	82.8	42.4	37.2	54	73.9	n.d.	61	42.9	118.2	73.4	69	91	99.1	n.d.
Sm	6.9	13.2	7.8	5.5	8.1	10.6	n.d.	8.4	7.8	17.6	12.7	12.8	13.7	15.2	n.d.
Eu	2.1	2.91	1.8	2.3	2.1	2.4	n.d.	1.9	2.3	2.3	2.4	4.1	2.4	3	n.d.
Gd	7.9	13.5	10.7	6.6	5.3	6.1	n.d.	5.1	10.1	11	17	16.4	9.9	11	n.d.
Tb	1	1.5	1.4	0.7	0.7	0.9	n.d.	0.8	1.3	1.5	2.1	2.1	1.3	1.6	n.d.
Dy	5.6	8.1	7.2	3.7	3.6	4.6	n.d.	4.1	7.2	8.4	11.6	11.2	6.8	8.5	n.d.
Ho	0.9	1.2	1.1	0.5	0.6	0.8	n.d.	0.8	1.1	1.5	1.6	1.6	1.2	1.5	n.d.
Er	2.5	3.4	3.2	1.7	1.7	2.3	n.d.	2.3	3.3	4.2	4.9	4.5	3.4	4.2	n.d.
Tm	0.4	0.5	0.4	0.3	0.2	0.3	n.d.	0.3	0.5	0.6	0.7	0.6	0.5	0.6	n.d.
Yb	2.4	3.1	3.1	1.7	1.5	2.1	n.d.	2.2	3.3	4.1	4.5	4	3.1	3.7	n.d.
Lu	0.4	0.5	0.5	0.3	0.2	0.3	n.d.	0.3	0.5	0.6	0.7	0.6	0.5	0.6	n.d.

	Phonolitic dykes with tinguaitic texture						Phonolite dykes		Alkali granite dyke				Carbonatitic dykes			
Sample	82317	70508	70510	70504	70509	70506	70516	70517	70514	82305	82309	70515	70503	71504	LG-07	LG-11
Cr	n.d.	n.d.	7	n.d.	n.d.	n.d.	n.d	n.d.	n.d.	7	5	n.d.	1	2	6.73	27.13
Ni	4	5	11	4	4	4	7	4	5	5	6	6	18	18	20.71	22.56
Rb	175	177	297	228	239	305	313	272	213	209	201	201	248	56.3	13.09	4.31
Ba	2396	2377	2541	128	463	92	541	222	646	516	496	643	2198	1677	31833	1426
Th	26	24	53	108	116	91	83	91	19	20	20	22	1397	1112	4.80	12.49
U	7.8	n.d.	5.9	34.8	17.6	33	n.d.	10.4	n.d.	n.d.	3.7	n.d.	114	48.8	4.37	6.84
Nb	32	n.d.	39.8	70.2	47.1	67.6	n.d.	46	n.d.	n.d.	9.6	n.d.	1	14.5	2.75	3.42
Ta	2.2	n.d.	2.9	5.4	4.5	3.6	n.d.	2.9	n.d.	n.d.	1.8	n.d.	0.1	0.4	0.19	0.20
Sr	2477	2438	2349	750	1002	438	600	562	317	282	416	408	2167	3883	1664	3188
Pb	63	64	119	61	64	198	142	159	20	22	23	23	1967	754	55.69	154.34
Zr	546	555	413	913	956	1051	621	787	179	177	176	182	175	129	47.19	18.34
Hf	8.3	n.d.	5.3	16.4	13.9	15	n.d.	13	n.d.	n.d.	4.3	n.d.	0.2	0.2	1.05	0.43
Y	31	32	30	30	56	8	48	44	30	30	30	30	233	241	85.60	135.21
La	101	n.d.	96	128	120	256	n.d.	96	n.d.	n.d.	31	n.d.	10621	10420	426.7	804.5
Ce	204	n.d.	189	286	223	418	n.d.	243.3	n.d.	n.d.	64.7	n.d.	15451	15413	740.2	1613.2
Pr	22.2	n.d.	21	30.9	23.1	31.7	n.d.	25.3	n.d.	n.d.	7.1	n.d.	1522	1453	86.5	199.3

Continued

Nd	77.1	n.d.	39.9	99.8	54.7	72.2	n.d.	87.2	n.d.	n.d.	28.1	n.d.	3500	3871	329.2	756.8
Sm	12.2	n.d.	7.7	11.7	9.5	4.4	n.d.	15	n.d.	n.d.	5.5	n.d.	458.6	406.0	49.9	101.5
Eu	3.4	n.d.	2.7	2.7	2.5	0.8	n.d.	3.3	n.d.	n.d.	0.6	n.d.	92.4	83.0	18.1	31.5
Gd	8.4	n.d.	9.9	14.8	13.4	12.6	n.d.	16.2	n.d.	n.d.	4.8	n.d.	677	518	42.9	72.2
Tb	1.2	n.d.	1.2	1.6	1.9	0.5	n.d.	2	n.d.	n.d.	0.7	n.d.	32	26.0	4.31	7.36
Dy	6.4	n.d.	6.6	8.4	10.8	2.6	n.d.	10.2	n.d.	n.d.	4.7	n.d.	180	182	17.89	26.03
Ho	1.2	n.d.	1	1.2	1.9	0.2	n.d.	1.5	n.d.	n.d.	0.9	n.d.	10.8	11.0	3.23	4.47
Er	3.2	n.d.	2.8	3.8	6.1	0.9	n.d.	4.5	n.d.	n.d.	2.9	n.d.	46.6	41.2	8.58	12.56
Tm	0.5	n.d.	0.4	0.6	1.1	0.1	n.d.	0.6	n.d.	n.d.	0.4	n.d.	4.3	4.6	0.82	1.25
Yb	3.1	n.d.	2.5	4.3	7.3	0.6	n.d.	4.3	n.d.	n.d.	2.8	n.d.	30	29.7	4.57	7.07
Lu	0.4	n.d.	0.4	0.7	1.1	0.1	n.d.	0.6	n.d.	n.d.	0.4	n.d.	4.1	4.0	0.61	0.94

Table 4. Trace element concentrations (ppm) for selected intrusive samples from Mushgai Khudag and Bayan Khoshuu complexes.

	Mushgai Khudag								Bayan Khoshuu							
	Intrusive			Effusive			Carbonatitic dykes		Intrusive						F-Carbonatitic vein (4/BK) and dyke (8/BK-02)	
Sample	80801	90601	90703	80410	80408	80307-3	3/MK	8/MK-01	90706	90707	90704	90708	90709	90710	4/BK	8/BK-02
Cr	n.d.	n.d.	12	n.d.	5	25	n.d.	8.13	71	62	31	42	27	16	n.d.	12.23
Ni	15	4	6	12	11	32	<20	12.62	62	56	38	46	40	27	26	5.15
Rb	178	136	97	110	109	88	3.9	0.41	87	89	108	94	96	110	1.5	2.57
Ba	2409	1934	3024	1994	2260	2462	750	5027	3892	3992	3757	4094	4778	4060	115540	9580
Th	67	27	14	n.d.	n.d.	n.d.	17.1	2.59	13	16	11	15	13	25	3843	11.02
U	n.d.	6	2.8	n.d.	n.d.	n.d.	11.5	8.89	5.5	3.4	n.d.	3.81	n.d.	6.8	68	5.57
Nb	n.d.	26.8	14.8	24	17	11	6.0	0.16	16.1	13.4	n.d.	18.27	n.d.	22.3	<0.5	0.40
Ta	n.d.	1.4	0.67	n.d.	n.d.	n.d.	<0.1	0.01	0.9	0.9	n.d.	1.04	n.d.	1.2	0.6	0.08
Sr	2465	2222	3508	3057	3733	2588	5680	26628	9006	5429	4542	5375	5771	4824	147272	39500
Pb	84	104	76	n.d.	n.d.	n.d.	8.0	149.87	73	70	65	69	68	80	107	52.85
Zr	703	709	331	233	127	169	244	10.91	368	406	461	434	362	574	0.7	4.86
Hf	n.d.	8.7	3.4	n.d.	n.d.	n.d.	<0.5	0.23	3	4	n.d.	3.92	n.d.	6.2	<0.5	0.53
Y	23	23	26	36	34	18	131	31.40	23	21	23	24	29	31	592	103.17
La	n.d.	150.4	152.3	n.d.	n.d.	n.d.	2517	1826.0	178.2	154	n.d.	183.87	n.d.	200	59830	309.9
Ce	n.d.	295	312	n.d.	n.d.	n.d.	2636	1620.0	350.2	287.8	n.d.	347.62	n.d.	458.34	120066	610.4
Pr	n.d.	29.8	35.2	n.d.	n.d.	n.d.	844	110.8	37.7	31.4	n.d.	37.84	n.d.	48.6	10818	76.3
Nd	n.d.	107	128.5	177	165	n.d.	773	288.4	143.7	76.3	n.d.	144.3	n.d.	175.4	39765	299.9
Sm	n.d.	14.9	18.9	28.1	34.6.	n.d.	91.4	22.0	20.7	13	n.d.	20.6	n.d.	24.5	2555	46.8
Eu	n.d.	3.4	5.0	n.d.	n.d.	n.d.	32.4	8.8	5.2	4.9	n.d.	5.26	n.d.	6.3	512	13.9
Gd	n.d.	8.2	11.2	n.d.	n.d.	n.d.	31.8	34.0	15.0	17.4	n.d.	14.16	n.d.	16.1	745	34.5
Tb	n.d.	1.0	1.3	n.d.	n.d.	n.d.	5.8	1.84	1.4	1.7	n.d.	1.27	n.d.	1.6	73	3.67
Dy	n.d.	4.7	6.1	n.d.	n.d.	n.d.	16.2	5.63	6.0	8.4	n.d.	5.68	n.d.	7.2	200	14.89
Ho	n.d.	0.8	1.0	n.d.	n.d.	n.d.	6.5	1.05	0.9	0.9	n.d.	0.9	n.d.	1.2	28	2.53
Er	n.d.	2.1	2.5	n.d.	n.d.	n.d.	4.8	3.23	2.5	2.7	n.d.	2.24	n.d.	3.0	46.6	6.25
Tm	n.d.	0.3	0.3	n.d.	n.d.	n.d.	0.5	0.32	0.3	0.3	n.d.	0.26	n.d.	0.4	3.3	0.62
Yb	n.d.	1.7	1.9	n.d.	n.d.	n.d.	1.9	2.07	1.7	1.9	n.d.	1.55	n.d.	2.4	19.8	3.18
Lu	n.d.	0.3	0.3	n.d.	n.d.	n.d.	0.4	0.29	0.3	0.3	n.d.	0.24	n.d.	0.3	1.65	0.39

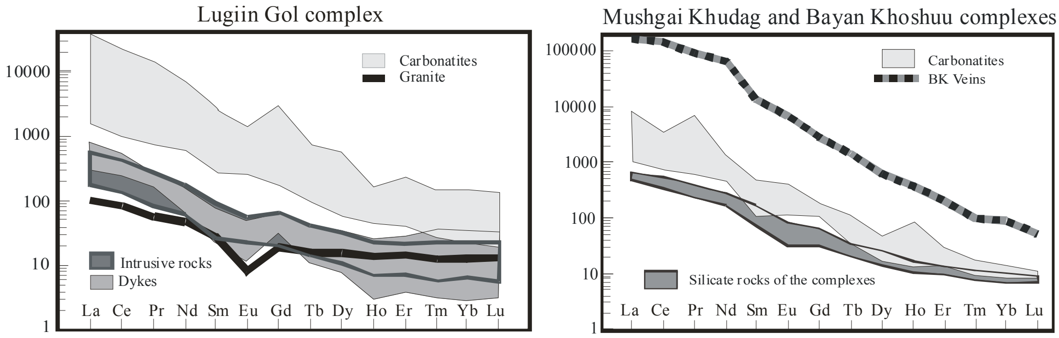

Figure 7. Chondrite normalized [35] REE pattern of the Lugiin Gol, Mushgai Khudag and Bayan Khoshuu complexes.

references).

5. Age of the Complexes

An errorchron calculated following the Rb/Sr systematics on the syenitic rocks from Lugiin Gol complex gives an age of 244.9 ± 22.4 Ma (initial Sr isotope ratio, Sr_i, = 0.70800; **Figure 8(a)**), roughly corresponding to “Sensitive High Resolution Ion Microprobe” (SHRIMP) ages (245 - 240 Ma) on the zircons from the same complex [19]. On the other hand, the whole rock-minerals isochron ages where determined for the three complexes by Rb-Sr method: $^{87}Rb/^{86}Sr$ and $^{87}Sr/^{86}Sr$ data are reported in **Table 5**. A Lugiin Gol undersaturated syenite sample shows an age of 222.2 ± 3.2 (2σ) Ma with Sr_i = 0.70811 ± 0.00009 (foid syenite 82306, **Figure 8(b)**); the Mushgai Khudag syenite (sample 90703) displays 139.9 ± 5.9 Ma and Sr_i = 0.70605 ± 0.00008 (**Figure 8(d)**); Bayan Khoshuu syenite (sample 90710) has an age = 130.6 ± 9.3 Ma with Sr_i = 0.70594 ± 0.00009 (**Figure 8(e)**).

Notably the Rb-Sr age from the isochron relative to the foid syenite from Lugiin Gol is too low (222 vs. 245 Ma) with respect to the whole complex: the younger age is probably due to the alteration processes that affected some host rocks after the intrusions of the dyke systems.

On the contrary, the Rb-Sr ages of the Mushgai Khudag and Bayan Khoshuu complexes are similar 1) to those reported by JICA [15] utilizing K-Ar systematic; and 2) to the Sm/Nd calculated ages (138 ± 3 and 134 ± 2, Mushgai Khudag and Bayan Khoshuu, respectively) .

An errorchron for the granitic dyke intruding the Lugiin Gol complex (cf. **Table 5**) gives an age of 209.9 ± 0.9 Ma (Sr_i = 0.70765; **Figure 8(c)**).

Moreover, an errorchron (not shown) relative to the whole rocks from Lugiin Gol foid syenites to foid-bearing syenites + associated phonolitic dykes and carbonatitic dyke, give the same age of the intrusive rocks, *i.e.* 244.9 ± 22.4 Ma. However this age, in our opinion, cannot be accepted because: 1) it is unlikely that the intruding dykes have the same age of the complex; 2) the Sm-Nd systematic does not show any correlation. An age younger than 222 Ma (probable age of hydrothermal alteration on the foid syenite 82306), or similar to that of the granitic dyke, *i.e.* 210 Ma, may be believed most probable also for phonolitic and carbonatitic dykes.

At any way, a Mesozoic age is confirmed, *i.e.* Triassic for Lugiin Gol complex, and Early Cretaceous for Mushgai Khudag and Bayan Khoshuu complexes.

6. Sr-Nd Systematics

All the available isotopic data, initial $^{87}Sr/^{86}Sr$ (Sr_i) - $^{143}Nd/^{144}Nd$ (Nd_i) and εSr - εNd notation are reported in **Table 6** along with the model age (T^{DM}) relative to the depleted mantle [38]. Lugiin Gol complex (calculated using the previous age results; cf. **Figure 8**) are in the ranges 0.70772 - 0.70827, 0.51216 - 0.51226 and 49.81 - 57.07, −4.24 - −1.25, respectively (syenitic variants: age 245 Ma); the phonolitic dykes (222 Ma) have Sr_i 0.70745 - 0.70888 and Nd_i 0.51220 - 0.51228, with εSr and εNd varying between 45.54 and 66.36, and between −3.02 and −1.73, respectively. The latter are similar to the carbonatitic dyke (εSr = 64.88 and εNd = −1.53). Notably, all these samples plot in the IV quadrant in the Sr_i vs. Nd_i diagram (**Figure 9**): according to [39] and therein references) these volcanics were enriched in Rb ($f_{Rb} > 0$) and depleted in Sm ($f_{Sm} < 0$), indicating that a hypothetical basalt source or may has formed by contamination by igneous and metamorphic rocks of the continental crust or, more probably remained isolated for a sufficient time to acquire distinctive isotopic composition of Sr and Nd.

The granitic dyke shows a slight enrichment in Nd (εNd + 0.48 to + 1.27), but with εSr (47.4 - 48.9) inside the same compositional variation of the phonolitic dykes, indicating a coupled enrichment in both Rb and Sm.

The Mushgai Khudag syenites-trachytes have, as average, Sr_i = 0.70605 ± 0.00001 and Nd_i = 0.51244, corresponding to εSr = 24.3 and εNd = −0.33, respectively (cf. **Table 6**).

Bayan Khoshuu syenites-monzonites show Sr_i = 0.70594 (εSr = 22.6), similar to the Mushgai Khudag volcanic-plutonic complex, but the Nd_i = 0.51224 (εNd = −4.4) indicate a major depletion in Sm in the source (**Figure 9**).

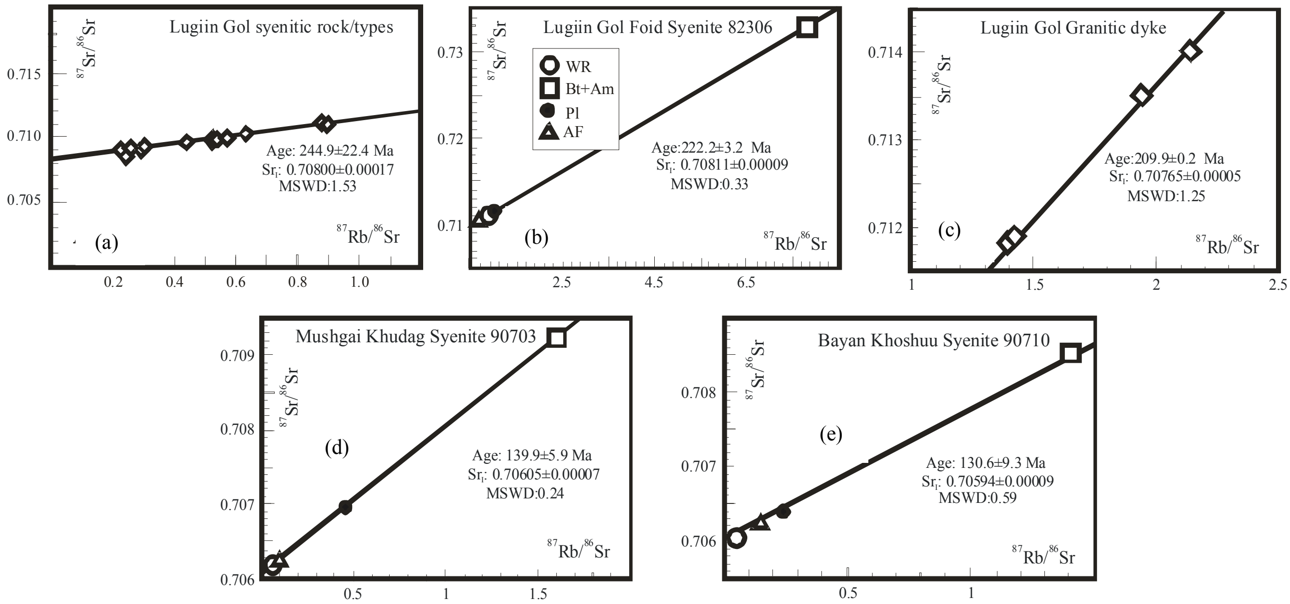

Figure 8. (a) Errorchron relative to the syenitic rocks (from foid syenites to foid bearing syenites) from Lugiin Gol complex; (b) Isochron for Lugiin Gol foid syenite 82306; (c) Errorchron for the samples from granitic dyke intruding the Lugiin Gol complex (cf. Tables 5 and 6); (d) Isochron for Mushgai Khudag syenite 90703; (e) Isochron for Bayan Khoshuu syenite 907010 ([36,37], unpublished data).

Table 5. ^{87}Rb/^{86}Sr and ^{87}Sr/^{86}Sr ratios for selected samples and minerals from Mongolian complexes (s. Table 6; cf. Figure 8).

Sample no.	^{87}Rb/^{86}Sr	^{87}Sr/^{86}Sr (2σ)	^{87}Sr/^{86}Sr	Sample no.	^{87}Rb/^{86}Sr	^{87}Sr/^{86}Sr (2σ)	^{87}Sr/^{86}Sr
Lugiin Gol Foid Syenite		measured	initial	**Mushgai Khudag** Syenite		measured	initial
82306 WR	0.8981	0.711022(11)	0.70816	90703 WR	0.080	0.706209(9)	0.70605
bt + amph	7.8253	0.732846(9)	0.70807	bt + amph	1.611	0.709250(8)	0.70605
plg	0.6906	0.710325(14)	0.70811	plg	0.461	0.706966(9)	0.70605
kfs	1.0815	0.711577(13)	0.70814	kfs	0.104	0.706267(9)	0.70606
Mean			0.70811				0.70605
Granitic dyke				**Bayan Khoshuu** Syenite			
70514 WR	1.9452	0.713511(9)	0.707702	90710 WR	0.066	0.706062(9)	0.70594
82305 WR	2.1456	0.714002(9)	0.707594	bt + amph	1.404	0.708544(7)	0.70594
82309 WR	1.3985	0.711814(9)	0.707638	plg	0.244	0.706393(8)	0.70595
70515 WR	1.4259	0.711890(10)	0.707632	kfs	0.141	0.706202(9)	0.70594
Mean			0.70764				0.70594

Although the rock-types of the examined complexes are strongly evolved, however the almost constant behaviour of the Sm/Nd ratio in the analyzed samples (^{147}Sm/^{144}Nd = 0.0100 ± 0.017) allows to consider the Nd model ages as indicative of the main metasomatic events affecting the lithospheric sources beneath the Mongolian regions. The model ages, calculated in relation to the depleted mantle (T^{DM}; cf. **Table 6**) for the whole population (33 samples) fit 992 ± 119 Ma, indicating a Neoproterozoic event ended with the Mushgai Khudag complex (797 ± 110 Ma), according to [41]. The latter dates are similar to the youngest Os model ages (1.1 and 0.7 - 0.5 Ga); [42] and may support significant melt extraction from the subcontinental mantle and/or metasomatic events.

7. Concluding Remarks

Alkaline complexes from southern Mongolia are controlled by E-W lineament. Mushgai Khudag (MKC) and Bayan Khoshuu (BAK) complexes are along the Main Mongolian lineament and Early Cretaceous aged (139 and 120 Ma, respectively). Notably carbonatitic stock

Table 6. Sr-Nd systematic relative to the examined complexes. Sr and Nd isotope ratios of whole rock samples and minerals and Rb, Sr, Sm and Nd contents of minerals were measured using a MAT 262 thermal ionization mass spectrometer equipped with five collectors. Initial $^{87}Sr/^{86}Sr$ and $^{143}Nd/^{144}Nd$ data were calculated as follows: Lugiin Gol, 245, 222, 210 Ma, syenitic facies, phonolitic-carbonatitic dykes, granitic dyke, respectively; Mushgai Khudag, 140 Ma; Bayan Khoshuu, 131 Ma. The values were determined according to [40]. T^{DM} values: calculation of Nd model dates relative to a depleted reservoir (*i.e.* $^{143}Nd/^{144}Nd$ = 0.513114 and $^{147}Sm/^{144}Nd$ = 0.222, after [39]).

Lugiin Gol

Sample no. LG-	Rb ppm	Sr ppm	$^{87}Rb/^{86}Sr$	$^{87}Sr/^{86}Sr$ (2) measured	$^{87}Sr/^{86}Sr$ initial	ε Sr	Nd ppm	Sm ppm	$^{147}Sm/^{144}Nd$	$^{143}Nd/^{144}Nd$ (2) measured	$^{143}Nd/^{144}Nd$ initial	ε Nd	T^{DM}
Foid syenites													
82308	226	1212	0.5396	0.709859(9)	0.70798	53.43	37.6	6.9	0.1109	0.512422(9)	0.512224	−1.53	1030
82313	204	1026	0.5754	0.709941(10)	0.70794	52.83	83.5	13.7	0.0992	0.512406(8)	0.512247	−1.48	948
82306	247	796	0.8981	0.711022(11)	0.70789	52.21	42.4	7.8	0.1107	0.512395(9)	0.512217	−2.07	1071
82302	174	2182	0.2307	0.708994(15)	0.70819	56.43	32.5	5.0	0.0924	0.512337(9)	0.512188	−2.63	986
82303	165	1792	0.2664	0.709163(10)	0.70823	57.07	54.0	8.1	0.0907	0.512385(9)	0.512239	−1.62	911
82315	200	1955	0.2960	0.708955(11)	0.70794	52.94	73.9	10.6	0.0867	0.512382(9)	0.512242	−1.55	888
82311	177	1686	0.3038	0.709231(9)	0.70827	56.19	35.1	5.6	0.0965	0.512260(9)	0.512243	−4.24	1109
82307	220	1211	0.5257	0.709967(12)	0.70813	55.65	61.0	8.4	0.0832	0.512362(9)	0.512229	−1.85	887
82314	160	1918	0.2414	0.708759(9)	0.70792	52.57	42.9	7.8	0.1104	0.512401(8)	0.512225	−1.91	1045
82304	223	1218	0.5298	0.709673(10)	0.70783	51.28	90.9	13.7	0.0911	0.512304(9)	0.512158	−3.21	968
Foid-bearing syenites													
82301	247	1119	0.6388	0.710269(9)	0.70804	54.35	118.2	17.6	0.0900	0.512386(9)	0.512242	−1.58	906
82312	241	791	0.8818	0.711082(15)	0.70801	53.87	73.4	12.7	0.1049	0.512401(10)	0.512233	−1.74	1001
70507	174	2037	0.2472	0.708585(9)	0.70772	49.81	69.0	13.0	0.1118	0.512390(9)	0.512207	−2.25	1105
82304	223	1218	0.5298	0.709673(10)	0.70783	51.28	90.9	13.7	0.0911	0.512304(9)	0.512158	−3.21	968
Monzonite													
82316	214	1394	0.4442	0.709605(11)	0.70806	54.55	99.1	15.2	0.0927	0.512407(9)	0.512258	−1.25	900
Phonolites													
82317	175	2477	0.2044	0.708095(9)	0.70745	45.54	77.7	12.2	0.0957	0.512383(21)	0.512245	−2.09	945
70508	177	2438	0.2101	0.708168(9)	0.70751	46.33	n.d.	n.d.					
70504	228	750	0.8798	0.711164(9)	0.70839	58.84	99.8	11.7	0.0708	0.512342(9)	0.512239	−2.21	834
70509	239	1002	0.6903	0.710612(9)	0.70843	59.50	54.7	9.5	0.1050	0.512416(9)	0.512263	−1.73	984
70506	305	438	2.0162	0.715246(9)	0.70888	65.85	58.2	3.9	0.0405	0.512320(9)	0.512261	−1.78	711
70510	297	2349	0.3659	0.709723(9)	0.70857	61.42	39.9	7.7	0.1161	0.512367(9)	0.512198	−3.02	1187
70516	313	600	1.5102	0.713684(9)	0.70892	66.36	66.5	13.0	0.1182	0.512395(21)	0.512223	−2.52	1144
70517	272	562	1.4010	0.713062(11)	0.70864	62.42	57.8	11.3	0.1182	0.512406(9)	0.512234	−2.30	1128
Carbonatite dyke													
70503	248	2167	0.3312	0.709857(8)	0.70881	64.88	3500	458.6	0.0792	0.512389(12)	0.512274	−1.53	1154
Alkali granite porphyry dike													
70514	213	317	1.9452	0.713511(9)	0.70770	48.93			0.1183	0.512564(17)	0.512401	0.66	891
82305	209	282	2.1456	0.714002(9)	0.70759	47.40			0.1183	0.512555(13)	0.512392	0.48	804
82309	201	416	1.3985	0.711814(9)	0.70764	48.01	28.1	5.5	0.1183	0.512593(9)	0.512430	1.22	847
70515	201	408	1.4259	0.711890(10)	0.70763	47.93							

Mushgai Khudag

Sample no.	Rb ppm	Sr ppm	$^{87}Rb/^{86}Sr$	$^{87}Sr/^{86}Sr$ (2) measured	$^{87}Sr/^{86}Sr$ initial	ε Sr	Nd ppm	Sm ppm	$^{147}Sm/^{144}Nd$	$^{143}Nd/^{144}Nd$ (2) measured	$^{143}Nd/^{144}Nd$ initial	ε Nd	T^{DM}
Syenites-Trachytes													
80801	178	2465	0.209	0.706465(7)	0.70605	24.33							
90601	136	2222	0.177	0.706407(8)	0.70606	24.34	107.0	14.9	0.084	0.512517(10)	0.512440	−0.35	718
90703	97	3508	0.080	0.706209(9)	0.70605	24.31	128.5	18.9	0.089	0.512522(11)	0.512440	−0.34	739
80410	110	3057	0.104	0.706257(7)	0.70605	24.31	177	28.1	0.096	0.512528(10)	0.512440	−0.35	774
80408	109	3733	0.084	0.706217(8)	0.70604	24.30	165	34.6	0.127	0.512556(12)	0.512440	−0.35	985

Bayan Khoshuu

Syenites-Monzonites													
90706	87	9006	0.028	0.705992(7)	0.70594	22.60	143.7	20.7	0.087	0.512324(9)	0.512249	−4.29	957
90707	89	5429	0.047	0.706027(7)	0.70594	22.58	76.3	13.0	0.103	0.512338(9)	0.512250	−4.29	1069
90708	94	5375	0.051	0.706037(6)	0.70594	22.64	144.3	20.6	0.109	0.512343(9)	0.512269	−3.91	929
90710	110	4824	0.066	0.706061(9)	0.70594	22.57	175.4	24.5	0.085	0.512322(7)	0.512250	−4.29	940

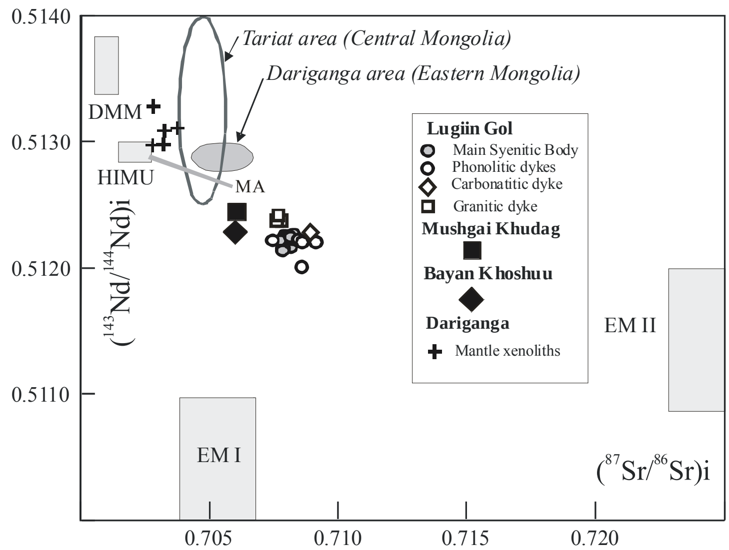

Figure 9. Time integrated ($^{87}Sr/^{86}Sr$)i vs (143Nd/144Nd)i for the Lugiin Gol, Mushgai Khudag and Bayan Khoshuu complexes. For the mantle components (DMM, HIMU, EMI and EMII) and Mantle Array (MA), s. [38,43-46]. Data sources for mantle xenoliths, Tariat and Dariganga areas: [42,47-49].

works are present in the two complexes. On the other hand, the Lugiin Gol (LGC) complex outcrops at the central-eastern Gobi-Tien Shan fold belt and it is Triassic in age (244 - 210 Ma). MKC and BAK consist mainly of slightly oversaturated syenites (monzonites) and trachytes, while in the LGC the rock-types are mainly foid-syenites and foid-bearing syenites and the complex is cut by a stockwork made of phonolitic and carbonatitic veins and dykes.

All the alkaline rocks are potassic, rarely highly potassic, and mainly intermediate silica-types, alkali granitic dyke excepted, and then they are believed derivative from a basic magma, probably a basanitic liquid, analogously to other world-wide occurrences and on the basis also of the trace element behavior ([50] and therein references); [32-34]; clinopyroxene and calcic plagioclase are evolving by fractional crystallization of olivine during ascent to the present position.

Stockworks of LREE rich carbonatites, carbonate-fluorite, fluorite, and carbonate-fluorite-celestine-barite REE ore bearing rocks are associated with the complexes and point to an economic interest of the region.

On the whole, geochemical characteristics of alkaline complexes in South Mongolia were interpreted as formed within-plate tectonic environment and associated with extensional rift tectonics [3].

All the samples plot in the IV quadrant in the Sri vs. Ndi diagram showed enrichment in Rb ($f_{Rb} > 0$) and depletion in Sm ($f_{Sm} < 0$), indicating that a hypothetical basalt probably remained isolated for a sufficient time to gain distinctive isotopic composition of Sr and Nd.

Finally, on the basis of almost constant behaviour of the Sm/Nd ratio in the analyzed samples ($^{147}Sm/^{144}Nd$ = 0.0100 ± 0.017), the Nd model ages can represent the main metasomatic events affecting the lithospheric sources beneath the Mongolian regions (veined lithospheric mantle). T^{DM} (**Table 6**) for the whole population (33 samples) fit 992 ± 119 Ma, indicating a Neoproterozoic event ended with the Mushgai Khudag complex (797 ± 110 Ma). The latter dates are similar to the youngest Os model ages (1.1 and 0.7 - 0.5 Ga) [42], and may support significant melt extraction from the subcontinental mantle or metasomatic events, suggesting also involvement of the Central Asian Orogenic belt and development of significant juvenile crustal growth.

8. Acknowledgements

We acknowledge Professor Yoshihiro Sawada for his support in XRF analyses, Professor Masahide Akasaka for providing and helping in EPMA and XRD analyses, Professor Jun-ichi Kimura for supporting in ICP-MS analyses, and also to Mrs. Akasaka for her help in preparing samples for isotope analyses. We also acknowledge A. R. Chakhmouradian, Cheng Xu, Hana Cihlarova, P. Gadas and R. Skoda for the acquisition of analytical data and support. Thank Mr. Kh. Enkhtuvshin and D. Batbold, Yo. Majigsuren for their help in field work.

Finally, we acknowledge for the financial support on Monbusho (Japanese Ministry of Education and Culture) and CEITEC CZ.1.05/1.1.002.0068, Czech Republic.

P.C.C. dedicates this paper to the memory of Enzo Michele Piccirillo.

REFERENCES

[1] B. A. Baskina, I. K. Volchanskaya, V. I. Kovalenko, *et al*., "Potassic Alkaline Volcanic-Plutonic Complex of Mushgai Khudag in South Mongolia and Related Mineralization," *Sovetskaya Geologiya*, No. 4, 1978, pp. 86-99 (in Russian).

[2] V. A. Baskina, I. K. Volchanskaya, V. I. Kovalenko, V. S. Samojlov, N. V. Vladykin, A. V. Goreglad, O. D. Suetenko and V. F. Shuvalov, "The Potassic Alkaline Volcanic-Plutonic Massif at Mushugai Khuduk in South Mongolia and Related Mineralization," *Sovetskaya Geologiya*, Vol. 4, 1978, pp. 86-99 (in Russian).

[3] V. S. Samoilov and V. I. Kovalenko, "Complexes of Alkaline Rocks and Carbonatites in South Mongolia," *Nauka*, Vol. 35, 1983, p. 196 (in Russian).

[4] D. Batbold, "Mineralogy of the Carbonatite from the Lugiin Gol Alkaline Pluton, South Mongolia," *Mongolian Geoscientist*, Vol. 8, 1998, p. 37.

[5] Kh. Enkhtuvshin, "A Petrological Study on the Late Mesozoic and Cenozoic Volcanic Rocks of the Mongolian Plateau," Master Thesis, Shimane University, 1995, p. 119.

[6] O. Gerel, B. Munkhtengel, H. Enkhtuvshin and D. Batbold, "Petrology and Geochemistry of the Mushgai Khudag Volcanic-Plutonic Complex," *Geology*, Vol. 4, 2001, pp. 51-58 (in Monglian).

[7] I. A. Andreeva, V. I. Kovalenko and V. B. Naumov, "Origin, Magma Content, and Genesis of Silicate Magma of Alkaline Carbonatite-Bearing Complex of Mushgai Khudag, South Mongolia," *Petrology*, Vol. 9, 2001, pp. 563-582 (in Russian).

[8] Q.-R. Meng, "What Drove Late Mesozoic Extension of the Northern China-Mongolia Tract?" *Tectonophysics*, Vol. 369, No. 3-4, 2003, pp. 155-174. http://dx.doi.org/10.1016/S0040-1951(03)00195-1

[9] J. V. Amory, M. S. Hendrix, M. Lamb, A. M. Keller, G. Badarch and O. Tomurtogoo, "Permian Sedimentation and Tectonics of Southern Mongolia. Implications for a Time-Transgressive Collision with North China," *Geological Society of America*, *Abstracts with Program*, Vol. 26, No. 7, 1994, p. 242.

[10] C. M. Han, M. Sun, S. F. Lin, H. L. Chen, Z. L. Li and J. L. Li, "NW China: Implications for the Tectonic Evolution of Central Asia," *Journal of Asian Earth Sciences*, Vol. 32, No. 2-4, 2008, pp. 102-117. http://dx.doi.org/10.1016/j.jseaes.2007.10.008

[11] J. Kynicky and P. Samec, "Hydrothermally-Metasomatic and Exsolution-Like Mineralization of the Carbonatites from the Selected Localities at Gobi," *Mongolian Geoscientist*, Vol. 27, 2005, pp. 52-56.

[12] D. Batbold, "Mineralogy of the Carbonatite from the Lugiin Gol Alkaline Pluton, South Mongolia," Master Thesis, Shimane University, Matsue, 1997, p. 210.

[13] V. I. Kovalenko, V. V. Yarmolyuk, I. A. Andreeva, N. A. Ashikhmina, A. M. Kozlovsky, E. A. Kudryashova, V. A. Kuznetsov, E. N. Listratova, D. A. Lykin and A. V. Nikiforov, "Part 2. Magma Types and Their Source in the History of the Earth. Rare Metal Magmatism: Rock Associations, Content and Magma Sources, Geodynamic Environment," *M. IGEM RAN*, 2006, p. 280.

[14] J. Kynicky, "Petrology of the Carbonatites from the Selected Localities at Gobi," Master Thesis, Masyryk University, Brno, 2002, p. 78.

[15] Japan International Cooperation Agency and Metal Mining Agency of Japan, "Report on the Mineral Exploration in Uudam-Tal Area," Mongolian People's Republic (Phase I), 1992.

[16] A. Streckeisen, "To Each Plutonic Rock Its Proper Name," *Earth Science Reviews*, Vol. 12, No. 1, 1976, pp. 1-33. http://dx.doi.org/10.1016/0012-8252(76)90052-0

[17] R. W. Le Maitre, Ed., "A Classification of Igneous Rocks and Glossary of Terms," Oxford, Blackwell, 1989, p. 193.

[18] J. Kynicky, C. Xu, A. R. Chakhmouradian, E. Reguir, H. Cihlářová and M. Brtnický, "REE Mineralization of High Grade REE-Ba-Sr and REE-Mo Deposits in Mongolia and China," *Mineralogical Magazine* (*Goldschmidt Abstracts*), Vol. 75, 2011, p. 1260.

[19] J. Kynicky, A. R. Chakhmouradian, C. Xu, M. Vašinová, M. Brtnický and M. Smith, "Origin and Evolution of the Lugiin Gol Carbonatites (Southern Mongolia) and Associated Rare-Earth Mineralization," *Ore Geology Reviews*, Vol. 53, 2013, in Print.

[20] J. Kynicky, "Primary and Secondary Minerals of Carbonatites of South Mongolia," *Mineral*, Vol. 11, 2003, pp. 57-61.

[21] J. Kynicky, "Carbonatites of South Mongolia," Dissertation Thesis, Mendel University, Brno, 2006, p. 181.

[22] P. Comin-Chiaramonti, C. B. Gomes, A. Cundari, F. Castorina and P. Censi, "A Review of Carbonatitic Magmatism in the Paraná-Angola-Etendeka (Pan) System," *Periodico di Mineralogia Ezio Callegari*, Vol. 76, 2007, pp. 25-78.

[23] M. J. Le Bas and R. W. Le Maitre, A. Streckeisen and B. Zanettin, "A Chemical Classification of Volcanic Rocks Based on the Total Alkali-Silica Diagram," *Journal of Petrology*, Vol. 27, No. 3, 1986, pp. 745-750. http://dx.doi.org/10.1093/petrology/27.3.745

[24] E. A. K. Middlemost, "Naming Materials in the Magma Igneous System," *Earth-Science Review*, Vol. 37, No. 3-4, 1994, pp. 215-224. http://dx.doi.org/10.1016/0012-8252(94)90029-9

[25] L. Beccaluva, M. Barbieri, H. Born, P. Brotzu, M. Coltorti, A. Conte, C. Garbarino, C. B. Gomes, G. Macciotta, L. Morbidelli, E. Ruberti, F. Siena and G. Traversa, "Frac-

tional Crystallization and Liquid Immiscibility Processes in the Alkaline-Carbonatite Complex of Juquiá (São Paulo, Brazil),” *Journal of Petrology*, Vol. 33, No. 6, 1992, pp. 1371-1404. http://dx.doi.org/10.1093/petrology/33.6.1371

[26] E. Ruberti, F. Castorina, P. Censi, P. Comin-Chiaramonti, C. B. Gomes, P. Antonini and F. Andrade, “The Geochemistry of the Barra do Itapirapuã Carbonatite (Ponta Grossa Arch, Brazil): A Multiple Stockwork,” *Journal of South America Earth Sciences*, Vol. 15, No. 2, 2002, pp. 215-228. http://dx.doi.org/10.1016/S0895-9811(02)00031-7

[27] T. N. Irvine and W. R. A. Baragar, “A Guide to the Chemical Classification of the Common Volcanic Rocks,” *Canadian Journal of Earth Sciences*, Vol. 8, No. 5, 1971, pp. 523-548. http://dx.doi.org/10.1139/e71-055

[28] R. W. Le Maitre, “Some Problems of the Projection of Chemical Data into Mineralogical Classifications,” *Contributions to Mineralogy and Petrology*, Vol. 56, No. 2, 1976, pp. 181-189. http://dx.doi.org/10.1007/BF00399603

[29] A. Streckeisen, “IUGS Subcommission on the Systematic of Igneous Rocks,” *Neues Jahrbuch für Mineralogie, Abhandungen*, Vol. 143, 1978, pp. 1-14.

[30] G. E. R. Gomes, C. B. Comin-Chiaramonti and P. Hydrothermal, “REE Fluorocarbonatite Mineralization at Barra do Itapirapuã, a Multiple Stockwork Carbonatite, Southern Brazil,” *Can Mineral*, Vol. 46, 2008, pp. 901-914. http://dx.doi.org/10.3749/canmin.46.4.901

[31] S.-S. Sun and W. F. McDonough, “Chemical and Isotopic Systematics of Oceanic Basalts: Implications for Mantle Composition and Processes,” In: A. D. Saunders and M. J. Norry, Eds., *Magmatism in the Ocean Basinsi Geological Society of London Sp.*, Vol. 42, 1989, pp. 313-345.

[32] P. Comin-Chiaramonti and C. B. Gomes, Eds., “Mesozoic to Cenozoic Alkaline Magmatism in the Brazilian Platform,” Edusp/Fapesp, São Paulo, 2005, p. 757.

[33] S. F. Foley, “Petrological Characterization of the Source Components of Potassic Magmas: Geochemical and Experimental Constraints,” *Lithos*, Vol. 28, No. 3-6, 1992, pp. 187-204.

[34] S. F. Foley, “Vein Plus Wall-Rock Melting Mechanism in the Lithosphere and Origin of Potassic Alkaline Magmas,” *Lithos*, Vol. 28, No. 3-6, 1992, pp. 435-453. http://dx.doi.org/10.1016/0024-4937(92)90018-T

[35] W. V. Boynton, “Cosmochemistry of the Rare Earth Elements: Meteorite Studies,” In: P. Henderson, Ed., *Rare Earth Element Geochemistry*, Elsevier, Amsterdam, 1984, pp. 63-114. http://dx.doi.org/10.1016/B978-0-444-42148-7.50008-3

[36] B. Munkhtsengel and S. Iizumi, “Rb-Sr Geochronology and Sr-Nd Isotope Systematics of the Mushgai Khudag Syenite and Bayan Khoshuu Monzonite in South Mongolia,” *Mongolian Geoscientist*, Vol. 14, 1999, pp. 14-16.

[37] B. Munkhtsengel and S. Iizumi, “Petrology and Geochemistry of the Lugiin Gol Nepheline Syenite Complex in the Gobi-Tien Shan Fold Belt, Southern Mongolia: A Post-Collisional Potassic Magmatism,” *Mongolian Geoscientist*, Vol. 14, 1999, pp. 12-14.

[38] A. Zindler and S. Hart, “Chemical Geodynamics,” *Annual Review of Earth and Planetary Sciences*, Vol. 14, 1986, pp. 493-471. http://dx.doi.org/10.1146/annurev.ea.14.050186.002425

[39] G. Faure, “Principles of Isotope Geology,” 2nd Edition, Wiley, New York, 1986.

[40] D. J. De Paolo, “Trace Element and Isotopic Effects of Combined Wallrock Assimilation and Fractional Crystallization,” *Earth and Planetary Science Letters*, Vol. 53, No. 2, 1981, pp. 189-202. http://dx.doi.org/10.1016/0012-821X(81)90153-9

[41] V. I. Kovalenko, V. V. Yarmolyuk, V. P. Kovach, A. B. Kotov, I. K. Kozakov, E. B. Salnikova and A. M. Larin, “Isotope Provinces, Mechanisms of Generation and Sources of the Continental Crust in the Central Asian Mobile Belt: Geological and Isotopic Evidence,” *Journal of Asian Earth Sciences*, Vol. 23, No. 5, 2004, pp. 605-627. http://dx.doi.org/10.1016/S1367-9120(03)00130-5

[42] L.-K. Wang, S. O’Reilly, V. Kovach, W. L. Griffin, N. J. Pearson, V. Yarmolyuk, M. I. Kuzmin, C.-J. Chieh, J. G. Shellnutt and Y. Izuka, “Microcontinents among the Accretionary Complexes of the Central Asia Orogenic Belt: *In Situ* Re-Os Evidence,” *Journal of Asian Earth Sciences*, Vol. 62, 2013, pp. 37-50. http://dx.doi.org/10.1016/j.jseaes.2011.09.016

[43] A. Zindler, E. Jagoutz and S. Goldstein, “Nd, Sr and Pb Isotopic Systematics in a Three-Component Mantle: A New Perspective,” *Nature*, Vol. 298, 1982, pp. 519- 523.

[44] S. R. Hart, D. C. Gerlach and W. M. White, “A Possible New Sr-Nd-Pb Mantle Array and Consequences for Mantle Mixing,” *Geochimica et Cosmochimica Acta*, Vol. 50, No. 7, 1986, pp. 1551-1557.

[45] S. R. Hart, “Heterogeneous Mantle Domains; Signatures, Genesis and Mixing Chronologies,” *Earth and Planetary Science Letters*, Vol. 90, No. 3, 1988, pp. 273-296. http://dx.doi.org/10.1016/0012-821X(88)90131-8

[46] B. L. Weaver, “The Origin of Ocean Island End-Member Compositions: Trace Element and Isotopic Constraints,” *Earth and Planetary Science Letters*, Vol. 104, No. 2-4, 1991, pp. 381-397. http://dx.doi.org/10.1016/0012-821X(91)90217-6

[47] M. A. Lamb and G. Badarch, “Paleozoic Sedimentary Basins and Volcanic-Arc Systems of Southern Mongolia: New Stratigraphic and Sedimentologic Constraints,” *International Geology Review*, Vol. 39, No. 6, 1997, pp. 542-576. http://dx.doi.org/10.1080/00206819709465288

[48] U. Wiechert, D. A. Ionov and K. H. Wedepohl, “Spinel Peridotite Xenoliths from the Atsagir-Dush Volcano, Dariganga Lava Plateau, Mongolia: A Record of Partial Melting and Cryptic Metasomatism in the Upper Mantle,” *Contributions to Mineralogy and Petrology*, Vol. 126, No. 4, 1997, pp. 345-364. http://dx.doi.org/10.1007/s004100050255

[49] D. Burianek, P. Hanzl, V. Erban, H. Gilikova and K. Bolormaa, “The Early Cretaceous Volcanic Activity in the Western Part of the Gobi-Altai Rift (Shiliing Nuruu, SW Mongolia),” *Journal of Geosciences*, Vol. 53, 2008, pp. 167-180.

[50] A. Peccerillo, “Potassic and Ultraotassic Rocks: Compositional Characteristics, Petrogenesis and Geologic Significance,” *Episodes*, Vol. 15, 1992, pp. 243-251.